

Beam energy dependence of the viscous damping of anisotropic flow

Roy A. Lacey,^{1,2,*} A. Taranenko,¹ J. Jia,^{1,3} D. Reynolds,¹ N. N. Ajitanand,¹ J. M. Alexander,¹ Yi Gu,¹ and A. Mwai¹

¹*Department of Chemistry, Stony Brook University,
Stony Brook, NY, 11794-3400, USA*

²*Physics Department, Stony Brook University,
Stony Brook, NY, 11794-3800*

³*Physics Department, Brookhaven National Laboratory,
Upton, New York 11973-5000, USA*

(Dated: June 11, 2018)

The flow harmonics $v_{2,3}$ for charged hadrons, are studied for a broad range of centrality selections and beam collision energies in Au+Au ($\sqrt{s_{NN}} = 7.7 - 200$ GeV) and Pb+Pb ($\sqrt{s_{NN}} = 2.76$ TeV) collisions. They validate the characteristic signature expected for the system size dependence of viscous damping at each collision energy studied. The extracted viscous coefficients, that encode the magnitude of the ratio of shear viscosity to entropy density η/s , are observed to decrease to an apparent minimum as the collision energy is increased from $\sqrt{s_{NN}} = 7.7$ to approximately 62.4 GeV; thereafter, they show a slow increase with $\sqrt{s_{NN}}$ up to 2.76 TeV. This pattern of viscous damping provides the first experimental constraint for η/s in the temperature-baryon chemical potential (T, μ_B) plane, and could be an initial indication for decay trajectories which lie close to the critical end point in the phase diagram for nuclear matter.

PACS numbers: 25.75.-q, 25.75.Dw, 25.75.Ld

Heavy ion collisions provide an important avenue for studying the phase diagram for Quantum Chromodynamics (QCD) [1–3]. The location of the phase boundaries and the critical end point (CEP), in the plane of temperature vs. baryon chemical potential (T, μ_B), are fundamental characteristics of this phase diagram [4]. Lattice QCD calculations suggest that the quark-hadron transition is a crossover at high temperature (T) and small μ_B or high collision energy ($\sqrt{s_{NN}}$) [5]. For larger values of μ_B or lower $\sqrt{s_{NN}}$ [6], several model calculations have indicated a first order transition [7, 8] and hence, the possible existence of a CEP. It remains an experimental challenge however, to validate many of the essential “landmarks” of the phase diagram, as well as to extract the properties of each QCD phase.

Anisotropic flow measurements are sensitive to initial conditions, the equation of state (EOS) and the transport properties of the medium. Consequently, they are key to ongoing efforts to delineate the $\sqrt{s_{NN}}$ or (T, μ_B) dependence of the transport coefficient η/s , of the hot and dense matter created in collisions at both the Relativistic Heavy Ion Collider (RHIC) and the Large Hadron Collider (LHC). The Fourier coefficients v_n are frequently used to quantify anisotropic flow as a function of particle transverse momentum p_T , collision centrality (cent) and $\sqrt{s_{NN}}$;

$$\frac{dN}{d\phi} \propto \left(1 + 2 \sum_{n=1} v_n \cos n(\phi - \psi_n) \right), \quad (1)$$

where ϕ is the azimuthal angle of an emitted particle, and ψ_n are the azimuths of the estimated participant event planes [9, 10]; $v_n = \langle \cos n(\phi - \psi_n) \rangle$, where the brackets

denote averaging over particles and events, for a given centrality and p_T at each $\sqrt{s_{NN}}$ [11].

The LHC v_n measurements at $\sqrt{s_{NN}} = 2.76$ TeV, allow investigations of η/s at high T and small μ_B ; they compliment the v_n measurements from the recent RHIC beam-energy scan (BES) which facilitates a study of η/s for the μ_B and T values which span the collision energy range $\sqrt{s_{NN}} = 7.7 - 200$ GeV. Here, it is noteworthy that there are currently no experimental constraints for the μ_B and T dependence of η/s , especially for the lower beam energies. At the CEP or close to it, anomalies in the dynamic properties of the medium can drive abrupt changes in transport coefficients and relaxation rates [12, 13]. Therefore, a study of v_n measurements which span the the full range of energies available at RHIC and the LHC, also provides an opportunity to search for characteristics in the $\sqrt{s_{NN}}$ [or (T, μ_B)] dependence of η/s which could signal the location of the CEP [12, 13].

An important prerequisite for such studies is a method of analysis which allows a consistent evaluation of the influence of viscous damping on the v_n measurements which span the full range of $\sqrt{s_{NN}}$ values. In prior work [20, 21], we have validated the acoustic nature of anisotropic flow and shown that the strength of the dissipative effects which influence the magnitude of $v_n(p_T, \text{cent})$, can be expressed as a perturbation to the energy-momentum tensor $T_{\mu\nu}$ [22];

$$\delta T_{\mu\nu}(n, t) = \exp(-\beta' n^2) \delta T_{\mu\nu}(0), \quad \beta' = \frac{2\eta}{3s} \frac{1}{\bar{R}^2} \frac{t}{T}, \quad (2)$$

where $t \propto \bar{R}$ is the expansion time, T is the temperature, $k = n/\bar{R}$ is the wave number (*i.e.* $2\pi\bar{R} = n\lambda$

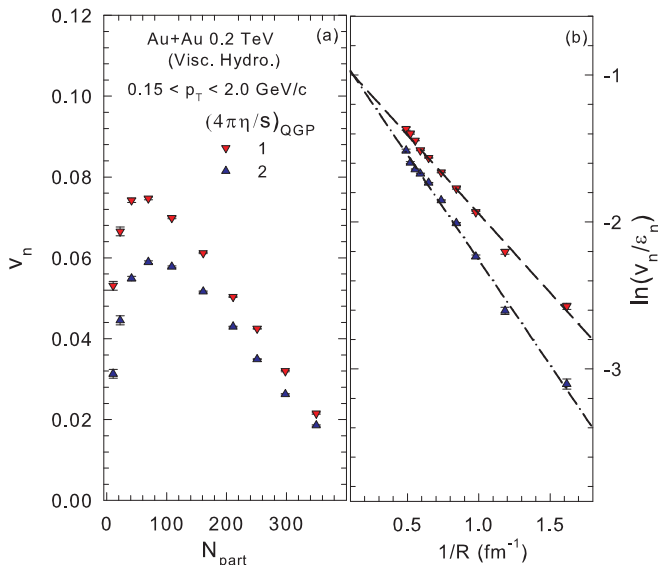


FIG. 1. (a) v_2 vs. N_{part} from viscous hydrodynamical calculations [14, 15] for two values of specific shear viscosity as indicated. The results are for $0.15 < p_T < 2.0$ GeV/c for Au+Au collisions at $\sqrt{s_{NN}} = 200$ GeV. (b) $\ln(v_n/\varepsilon_n)$ vs. $1/\bar{R}$ for the v_2 values shown in (a). The dashed and dot-dashed curves are linear fits.

for $n \geq 1$), \bar{R} is the initial state transverse size of the collision zone and $\delta T_{\mu\nu}(n, 0)$ represent the spectrum of initial ($t = 0$) perturbations associated with the collision geometry and its density driven fluctuations. The latter is encoded in the initial eccentricity (ε_n) moments. The viscous corrections to v_n/ε_n grow exponentially as n^2 and $1/\bar{R}$ [20, 21, 23];

$$\ln\left(\frac{v_n(\text{cent})}{\varepsilon_n(\text{cent})}\right) \propto \frac{-\beta''}{\bar{R}}, \quad \beta'' = \frac{4n^2\eta}{3Ts}, \quad (3)$$

For a given n , Eq. 3 indicates a characteristic linear dependence of $\ln(v_n/\varepsilon_n)$ on $1/\bar{R}$, with slope $\beta'' \propto \eta/s$. This scaling pattern is borne out in the results of the viscous hydrodynamical calculations [14, 15] shown in Fig. 1. The scaled results, shown for two separate values of η/s in Fig. 1(b), not only indicate a linear dependence of $\ln(v_n/\varepsilon_n)$ on $1/\bar{R}$, but also a clear sensitivity of the slopes to η/s . Thus, the validation of this $1/\bar{R}$ scaling for each beam energy, would provide a basis for consistent study of the $\sqrt{s_{NN}}$ dependence of the viscous coefficient β'' [12, 13, 24]. Here, we perform such validation tests for the full range of energies available at RHIC and the LHC, with an eye towards establishing new constraints for the $\sqrt{s_{NN}}$ or (μ_B, T) dependence of η/s .

The data employed in our analysis are taken from measurements by the ATLAS and CMS collaborations for Pb+Pb collisions at $\sqrt{s_{NN}} = 2.76$ TeV [18, 19, 25], as well as measurements by the STAR collaborations for Au+Au collisions spanning the range $\sqrt{s_{NN}} = 7.7 - 200$ GeV [16, 17, 26]. The ATLAS and CMS measurements

exploit the event plane analysis method and/or the two-particle $\Delta\phi$ correlation technique to obtain $v_n(p_T, \text{cent})$. To suppress the non-flow correlations, a pseudo-rapidity gap ($\Delta\eta_p$) between particles and the event plane, or particle pairs was used. The STAR measurements were obtained with several analysis methods for $\sqrt{s_{NN}} = 7.7 - 39$ GeV and the Q-cumulant method for $\sqrt{s_{NN}} = 62.4$ and 200 GeV. For purposes of consistency across beam energies, we use the data from the event plane analysis method ($v_2\{\text{EP}\}$) for $\sqrt{s_{NN}} = 7.7 - 39$ GeV, and the Q-cumulant method ($v_2\{2\}$) for $\sqrt{s_{NN}} = 62.4$ and 200 GeV. Note that the measurements from both analysis methods have been shown to be in good agreement for $\sqrt{s_{NN}} = 7.7 - 39$ GeV [26]. The systematic errors, which are relatively small, are reported in Refs. [18, 25] and [16, 17, 26] for the respective sets of measurements.

Monte Carlo Glauber (MC-Glauber) simulations were used to compute the number of participants $N_{\text{part}}(\text{cent})$, participant eccentricity $\varepsilon_n(\text{cent})$ [with weight $\omega(\mathbf{r}_\perp) = \mathbf{r}_\perp^n$] (and $\varepsilon_n\{2\}(\text{cent})$) and $\bar{R}(\text{cent})$ from the two-dimensional profile of the density of sources in the transverse plane $\rho_s(\mathbf{r}_\perp)$ [27]; $1/\bar{R} = \sqrt{(1/\sigma_x^2 + 1/\sigma_y^2)}$, where σ_x and σ_y are the respective root-mean-square widths of the density distributions. The initial state geometric quantities so obtained, are in excellent agreement with the values reported for Pb+Pb collisions at $\sqrt{s_{NN}} = 2.76$ TeV [25] and Au+Au collisions for the range $\sqrt{s_{NN}} = 7.7 - 200$ GeV [17, 26]. A centrality independent systematic uncertainty estimate of 2-3% was obtained for \bar{R} and ε respectively, via variations of the MC-Glauber model parameters. We use the values of \bar{R} and ε in concert with the RHIC and LHC data sets to perform validation tests for $1/\bar{R}$ scaling over the centrality selections of 5-70%, for each of the available beam energies.

Figures 2(a) and (c) show representative plots of $v_{2,3}$ vs. N_{part} for Au+Au and Pb+Pb collisions respectively. They show that $v_{2,3}$ increases from central ($N_{\text{part}} \sim 340$) to mid-central ($N_{\text{part}} \sim 120$) collisions as would be expected from an increase in $\varepsilon_{2,3}$ over the same N_{part} range. For $N_{\text{part}} \lesssim 120$ however, the decreasing trend of $v_{2,3}$ contrasts with the known increasing trends for $\varepsilon_{2,3}$, suggesting that the viscous effects due to the smaller systems produced in peripheral collisions, serve to suppress $v_{2,3}$. This is confirmed by the symbols and dashed curves in Figs. 2(b) and (d) which validate the expected linear dependence of $\ln(v_n/\varepsilon_n)$ on $1/\bar{R}$ (cf. Eq. 3) for the data shown in Figs. 2(a) and (c). Note that the slopes for $n = 3$ are more than a factor of two larger than those for $n = 2$ as expected (cf. Eq. 3). A similar dependence was observed for other p_T selections.

Validation tests for this $1/\bar{R}$ scaling of v_2 were carried out for the full range of available beam energies as illustrated in Fig. 3. Figs. 3(a)-(f) show p_T -integrated v_2 vs. N_{part} for a representative set of these collision energies as indicated; they show the same characteristic pattern ob-

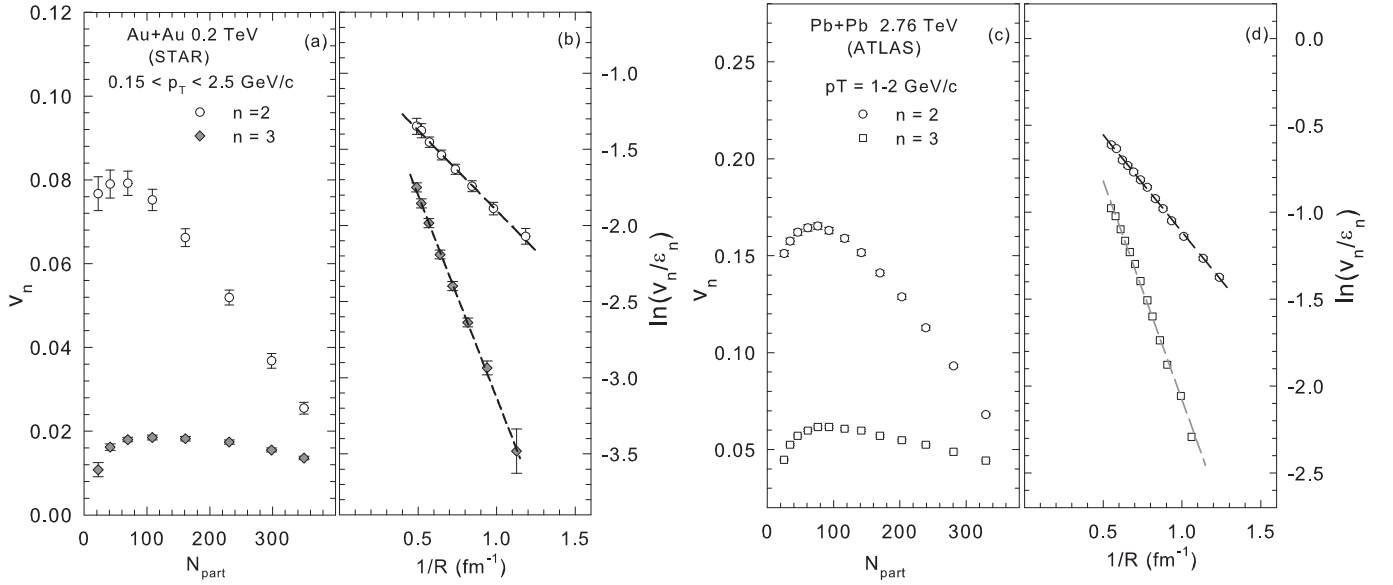


FIG. 2. (a) p_T -integrated $v_{2,3}$ vs. N_{part} for $0.15 < p_T < 2.5$ GeV/c for Au+Au collisions at $\sqrt{s_{NN}} = 200$ GeV. The $v_{2,3}$ data are taken from Refs. [16, 17]; (b) $\ln(v_n/\varepsilon_n)$ vs. $1/\bar{R}$ for the data shown in (a); (c) $v_{2,3}$ vs. N_{part} for Pb+Pb collisions at $\sqrt{s_{NN}} = 2.76$ TeV. The latter data are taken from Refs. [18, 19]; (d) $\ln(v_n/\varepsilon_n)$ vs. $1/\bar{R}$ for the data shown in (c). The dashed curves in (b) and (d) are fits to the data (see text); error bars are statistical only.

served for v_2 in Figs. 2(a) and (c). That is, the increase in v_2 from central to mid-central collisions, followed by a decrease for peripheral collisions, persists across the full range of collision energies. We interpret this as an indication that the transverse size of the collision zone plays a similar mechanistic role in viscous damping across the full range of beam energies studied. This is further confirmed in Figs. 3(a') – (f') which show the expected linear dependence of $\ln(v_n/\varepsilon_n)$ vs. $1/\bar{R}$, for the data shown in Figs. 3(a)-(f). A similar dependence was observed for the other collision energies ($\sqrt{s_{NN}} = 11.5, 27$ and 130 GeV) not shown in Fig. 3. This pervasive pattern of scaling provides the basis for a consistent method of extraction of the viscous coefficient $\beta'' \propto \eta/s$, via linear fits to the scaled data for each beam energy. The dashed curves in Figs. 3(a') – (f') show representative examples of such fits. The β'' values, with statistical errors obtained from these fits, are summarized in Fig. 4.

Figure 4 indicates only a mild variation in the magnitude of β'' for the broad span of collision energies studied (note the factor of ~ 360 increase from RHIC BES to LHC). This variation is compatible with the observation that v_2 measurements, obtained at different $\sqrt{s_{NN}}$, show similar magnitudes. That is, a larger variation of these coefficients would necessitate a much larger variation in the v_2 values obtained at different values of $\sqrt{s_{NN}}$, because of viscous damping. A more striking feature of Fig. 4 is the $\sqrt{s_{NN}}$ dependence of β'' . It shows that β'' decreases as $\sqrt{s_{NN}}$ increases from 7.7 GeV to approximately 62.4 GeV, followed by a relatively slow increase from $\sqrt{s_{NN}} = 62.4$ GeV - 2.76 TeV. Here, it should be

emphasized that the error bars for the extractions made at $62.4, 130$ and 200 GeV, as well as a lack of measurements between 39 and 62.4 GeV, do not allow a definitive estimate of the actual location of this apparent minimum. Nonetheless, we interpret this trend as an indication for the change in $\langle \eta/s \rangle$ which results from the difference in the decay trajectories sampled [in the (T, μ_B) plane] at each collision energy [12, 13]. A similar qualitative pattern of viscous damping has been recently obtained in transport calculations [28], as well as to reconcile the similarity between charged hadron $v_2(p_T)$ measurements obtained for $\sqrt{s_{NN}} > 62.4$ GeV [29].

The characteristic $\sqrt{s_{NN}}$ dependence of β'' shown in Fig. 4, also bears a striking resemblance to the T and μ_B dependence of η/s for atomic and molecular substances, which show η/s minima with a cusp at the critical end point $(T_{\text{cep}}, \mu_B^{\text{cep}})$ [12, 13]. Thus, the observed trend of the $\sqrt{s_{NN}}$ dependence of β'' could also be an indication for decay trajectories which lie close to the CEP. Further detailed extractions of β'' , with reduced error bars, are however required to pin point the apparent minimum and to further confirm its relationship to a possible CEP.

In summary, we have presented a detailed phenomenological study of viscous damping of the flow harmonics $v_{2,3}$ for Pb+Pb collisions at $\sqrt{s_{NN}} = 2.76$ TeV, and for Au+Au collisions spanning the range $\sqrt{s_{NN}} = 7.7 - 200$ GeV. Our study shows that this damping can be understood to be a consequence of the acoustic nature of anisotropic flow. That is, it validates the characteristic signature expected for the system size dependence of viscous damping [at each collision energy] inferred from the

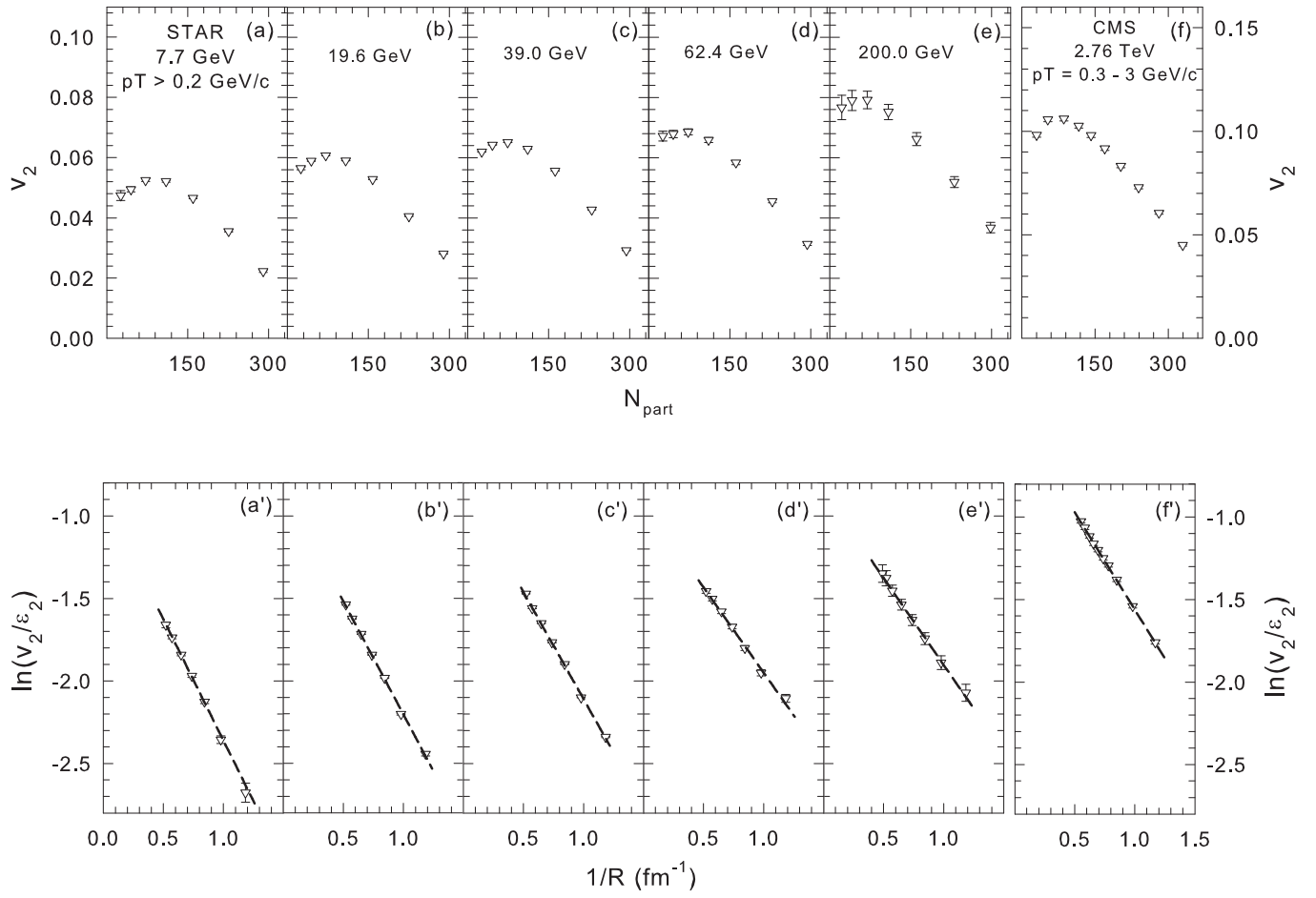


FIG. 3. ((a)-(e)) p_T -integrated v_2 vs. N_{part} for $p_T \gtrsim 0.2$ GeV/c for Au+Au collisions for several values of $\sqrt{s_{NN}}$ as indicated. The data are taken from Refs. [17, 26]: (f) v_2 vs. N_{part} for $p_T = 0.3 - 3$ GeV/c for Pb+Pb collisions at $\sqrt{s_{NN}} = 2.76$ TeV. These data are taken from Ref. [25]: ((a') - (f')) $\ln(v_2/\epsilon_2)$ vs. $1/\bar{R}$ for the data shown in (a)-(f). The dashed curves are linear fits to the data; error bars are statistical only.

218 dispersion relation for sound propagation in the matter
 219 produced in the collisions. The extracted viscous coeffi-
 220 cients, which encode the magnitude of the ratio of shear
 221 viscosity to entropy density η/s , are observed to decrease
 222 to an apparent minimum as the collision energy is in-
 223 creased from $\sqrt{s_{NN}} = 7.7$ to 62.4 GeV, albeit with a
 224 sizeable error; thereafter, it shows a slow increase with
 225 $\sqrt{s_{NN}}$. This pattern of viscous damping provides a first
 226 indication for the variation of η/s in the temperature-
 227 baryon chemical potential (T, μ_B) plane. It also bears a
 228 striking resemblance to the observations for atomic and
 229 molecular substances, which show η/s minima with a
 230 cusp at the critical end point ($T_{\text{cep}}, \mu_B^{\text{cep}}$). Further de-
 231 tailed studies, with improved errors and other harmonics,
 232 are required to make a more precise mapping of viscous
 233 damping in the (T, μ_B)-plane, as well as to confirm if the
 234 observed pattern for $\beta''(\sqrt{s_{NN}})$ reflects decay trajec-
 235 tories close to the critical end point in the phase diagram
 236 for nuclear matter.

237 **Acknowledgments:** This research is supported by

238 the US DOE under contract DE-FG02-87ER40331.A008
 239 and by the NSF under award number PHY- 1019387

* E-mail: Roy.Lacey@Stonybrook.edu

- [1] N. Itoh, Prog. Theor. Phys. **44**, 291 (1970).
- [2] E. V. Shuryak, CERN-83-01, CERN-YELLOW-83-01 (1983).
- [3] M. A. Stephanov, K. Rajagopal, and E. V. Shuryak, Phys.Rev.Lett. **81**, 4816 (1998), arXiv:hep-ph/9806219 [hep-ph].
- [4] M. SASakawa and K. Yazaki, Nucl. Phys. A **504**, 668 (1989).
- [5] Y. Aoki, G. Endrodi, Z. Fodor, S. Katz, and K. Szabo, Nature **443**, 675 (2006), arXiv:hep-lat/0611014 [hep-lat].
- [6] The baryon chemical potential increases with the decrease in the beam energy while the chemical freeze-out temperature increases with increase in beam energy [30].
- [7] S. Ejiri, Phys.Rev. **D78**, 074507 (2008),

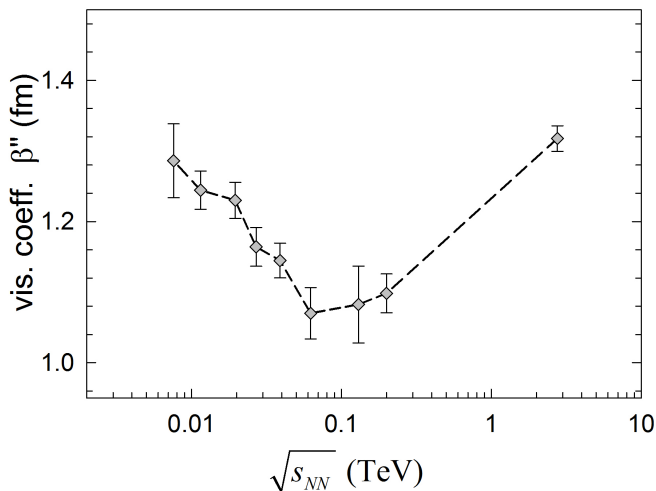


FIG. 4. Viscous coefficient β'' vs. $\sqrt{s_{NN}}$, extracted from linear fits to $\ln(v_2/\varepsilon_2)$ vs. $1/R$; error bars are statistical only. The dashed curve is drawn to guide the eye.

256 arXiv:0804.3227 [hep-lat].

257 [8] M. A. Stephanov, Int. J. Mod. Phys. A **20**, 4387 (2005).

258 [9] J.-Y. Ollitrault, Phys. Rev. **D46**, 229 (1992).

259 [10] A. Adare *et al.* (PHENIX),
260 Phys. Rev. Lett. **105**, 062301 (2010),
261 arXiv:1003.5586 [nucl-ex].

262 [11] Note that event-by-event fluctuations of the participant
263 c.m. rapidity can be significant, especially in peripheral
264 collisions [31].

265 [12] L. P. Csernai, J. Kapusta, and L. D.
266 McLerran, Phys.Rev.Lett. **97**, 152303 (2006),
267 arXiv:nucl-th/0604032 [nucl-th].

268 [13] R. A. Lacey, N. Ajitanand, J. Alexander, P. Chung,
269 J. Jia, *et al.*, (2007), arXiv:0708.3512 [nucl-ex].

270 [14] The v_2 values for MC-Glauber initial conditions, are ob-
271 tained from Fig. 6 or Ref. [15].

272 [15] H. Song, S. A. Bass, U. Heinz, T. Hirano,
273 and C. Shen, Phys.Rev. **C83**, 054910 (2011),
274 arXiv:1101.4638 [nucl-th].

275 [16] L. Adamczyk *et al.* (STAR Collaboration), (2013),
276 arXiv:1301.2187 [nucl-ex].

277 [17] G. Agakishiev *et al.* (STAR Collabo-
278 ration), Phys.Rev. **C86**, 014904 (2012),
279 arXiv:1111.5637 [nucl-ex].

280 [18] G. Aad *et al.* (ATLAS Collabora-
281 tion), Phys.Rev. **C86**, 014907 (2012),
282 arXiv:1203.3087 [hep-ex].

283 [19] J. Jia, J.Phys. **G38**, 124012 (2011),
284 arXiv:1107.1468 [nucl-ex].

285 [20] R. A. Lacey, Y. Gu, X. Gong, D. Reynolds, N. Ajitanand,
286 *et al.*, (2013), arXiv:1301.0165 [nucl-ex].

287 [21] R. A. Lacey, A. Taranenko, N. Ajitanand, and J. Alexan-
288 der, (2011), arXiv:1105.3782 [nucl-ex].

289 [22] P. Staig and E. Shuryak, (2010),
290 arXiv:1008.3139 [nucl-th].

291 [23] E. Shuryak and I. Zahed, (2013),
292 arXiv:1301.4470 [hep-ph].

293 [24] A. Bonasera and L. Csernai,
294 Phys.Rev.Lett. **59**, 630 (1987).

295 [25] S. Chatrchyan *et al.* (CMS Collabo-
296 ration), Phys.Rev. **C87**, 014902 (2013),
297 arXiv:1204.1409 [nucl-ex].

298 [26] L. Adamczyk *et al.* (STAR collabo-
299 ration), Phys.Rev. **C86**, 054908 (2012),
300 arXiv:1206.5528 [nucl-ex].

301 [27] R. A. Lacey, R. Wei, N. N. Ajitanand, and A. Taranenko,
302 (2010), arXiv:1009.5230 [nucl-ex].

303 [28] V. Ozvenchuk, O. Linnyk, M. Gorenstein,
304 E. Bratkovskaya, and W. Cassing, (2012),
305 arXiv:1212.5393 [hep-ph].

306 [29] S. Plumari, V. Greco, and L. Csernai, (2013),
307 arXiv:1304.6566 [nucl-th].

308 [30] J. Cleymans, H. Oeschler, K. Redlich,
309 and S. Wheaton, J.Phys. **G32**, S165 (2006),
310 arXiv:hep-ph/0607164 [hep-ph].

311 [31] V. Vovchenko, D. Anichishkin, and L. Csernai, (2013),
312 arXiv:1306.5208 [nucl-th].